# An approach using Dempster-Shafer Theory to fuse spatial data and satellite image derived crown metrics for estimation of forest stand leading species

Brice Mora[a], Michael A. Wulder[a], and Joanne C. White[a]

Affiliation:

[a] Canadian Forest Service, Pacific Forestry Centre, Natural Resources Canada, Victoria, BC, V8Z 1M5, Canada

Submitted to: Information Fusion

**Pre-print of published version.**
**Reference**:
Mora, B., M.A. Wulder, J.C. White. (2013). An approach using Dempster-Shafer Theory to fuse spatial data and satellite image derived crown metrics for estimation of forest stand leading species. Information Fusion. Vol. 14, No. 4. pp. 384-395.

**DOI**.
http://dx.doi.org/10.1016/j.inffus.2012.05.004
**Full text:**
http://www.sciencedirect.com/science/article/pii/S1566253512000577

**Abstract**

Leading species at the forest stand level is a required forest inventory attribute. Information regarding leading species enables the calculation of volume and biomass in support of forest monitoring and reporting activities. In this study, approaches for leading species estimation based upon very high spatial resolution (pixel sided < 1m) have been developed and implemented, with opportunities for improving attribute accuracy using data fusion methods. Over a study region located in the Yukon Territory, Canada, we apply the Dempster-Shafer Theory (DST) to integrate multiple resolutions of satellite imagery (including spatial and spectral), topographic information, and fire disturbance history records for the estimation of leading species.

Among the data source combinations tested in the study, the QuickBird panchromatic combined with selected optical channels from Landsat-5 Thematic Mapper (TM) imagery provided the highest overall accuracy (70.4%) for identifying leading species and improved the accuracy by 3.1% over a baseline from a classification-tree based method applied on all data sources. Additional insights to the application of DST to fuse satellite imagery with ancillary data sources to map leading stand species in a boreal environment are also elaborated upon, including the range and distribution of training data and DST mass function establishment.

Keywords: mapping, satellite imagery, evidential reasoning, landscape, forest, tree crown object metrics

## 1. Introduction

### *1.1. Context*

In forestry, the leading species in a stand is usually defined as the tree species with the highest proportion in terms of basal area. The identification of stand leading species is required to estimate stand volume and biomass [1], [2]. Forests and other wooded lands cover over 40% of Canada landmass [3], with forest dominated ecosystems representing approximately 60% of the national land base [4]. The National Forest Inventory (NFI) is based on a multiphase, plot-based framework designed to provide a 1% systematic sample of Canada's landmass. For the first phase of the inventory, over 19,000 photo plots 2 by 2 km in size and located on a 20 by 20 km grid have been used. Following installation and reporting of the first iteration of this sample plot based NFI [5], update of the NFI is now ongoing. The development of alternate data sources and processing methods [6], [7] is also underway to enable data collection and characterizations over remote areas or those areas not captured with provincial or territorial inventory programs. Very High Spatial Resolution (VHSR, <1 m) imagery offers a flexible means for data collection and opportunities for automated generation of forest stand attributes [2].

Mora et al. [6] proposed a method to identify stand leading species over a boreal environment, using information extracted from panchromatic QuickBird imagery (0.6 m spatial resolution). The method was based on a series of classification trees [8] and provided an overall accuracy of 72.5% with species accuracies ranging from 44% to 100%. Opportunities for incorporation of ancillary information sources that could improve the classification outcomes were envisioned, with topographic and disturbance information expected to add additional differentiation capacity. A linkage between disturbance history and species is also known, with fire history records informing on tree species-linked regeneration regimes.

The objective of this study is to investigate the capacity of a multi-source classification approach to improve upon classification accuracy of stand leading species compared to a conventional method. This work is based on the expectation that the Dempster-Shafer Theory (DST) [9], [10] is a suitable framework to combine heterogeneous data sources of information such as satellite imagery, topographic parameters, and spatial fire history records. We therefore posit that the precision of topographic and fire history records are sufficiently high to enable an efficient modelling of their influence on the spatial distribution of species present over the study area.

### *1.2. Methodological background*

Moisen and Frescino [11] used classification trees to predict broad forest classes (i.e., spruce-fir and woodland) in Montana and Arizona, USA. The predictor variables included elevation, aspect, slope, spectral bands from the Advanced Very High Resolution Radiometer (AVHRR) sensor, and a vegetation cover map derived from Landsat-5 Thematic Mapper (TM) imagery. Tree species were predicted for forested areas in Wyoming and Idaho, USA, with classification trees using Landsat-7 Enhanced Thematic Mapper Plus (ETM+) imagery, with elevation, aspect and slope as predictors [12]. Aertsen et al. [13] used classification trees to predict site index, a measure of site productivity, in Mediterranean mountain forests. Soil, vegetation, and topographical variables were used as inputs. In these studies classification trees along with regression

trees, were found to be efficient at selecting the best predictor variables and provide satisfying results for some attributes but the method was also defined as too simple to describe some real-world situations [13], [14].

Other classification procedures such as neural networks [15], Bayesian inference [16], fuzzy sets [17], and those referred to as evidential reasoning methods [18], have a demonstrated capacity to fuse heterogeneous (i.e., categorical or numerical) sources of information. Among the aforementioned procedures, the DST is a generalization of the Bayesian theory of subjective probability [16]. The strength of the DST is based upon a capacity to explicitly uncertainty and vagueness associated with the data to be fused. As opposed to classification trees, the DST enables the consideration of union classes (e.g., "black spruce OR trembling aspen"), along with singleton classes (e.g., "black spruce", "trembling aspen"). Note that uncertainty refers to the probability of an event occurring, while vagueness relates to the accuracy of an observation or measurement. The DST has the capacity to provide accurate results when the degree of conflict between the sources of information is limited, that is, when the input data sources do not provide contradictory information. Indeed, as shown by Zadeh [19], the DST can produce counter-intuitive results when data sources provide contradictory inputs. Some authors have proposed avenues to address and mitigate conflict between predictor data sources. The possibility theory first introduced by Zadeh [20], and further developed by Dubois and Prade [21], defined a disjunctive combination rule that allows the redistribution of the global conflict to the ignorance (union of classes). Smets [22] proposed the transferable belief model with a non-normalized combination rule that adheres to the *open-world* assumption. Smarandache and Dezert [23] proposed a non- normalized combination rule associated to a super power set that includes not only singleton and union classes but intersection classes as well.

Few applications of the DST have demonstrated the added value of the method for forest mapping, which manifests as an improvement of the overall classification accuracies compared to classical methods. Some recent examples include, Mora et al. [24], who fused SPOT-5 imagery with topographical information to map regenerating stands in southern Quebec, Canada (+7.4% compared to a maximum likelihood (ML) classifier). Cayuela et al. [25] fused a vegetation type map derived from Landsat-7 ETM+ with altitude, slope, and human settlement maps, for land-cover mapping in the Highlands of Chiapas, southern Mexico (+7.5% compared to a ML classifier). Franklin et al. [26] fused Landsat-5 TM imagery with DEM and forest inventory information to map grizzly bear habitat in Alberta, Canada (+14% compared to a ML classifier). Varma et al. [27] designed a DST-based decision support system for sustainable forest management. The proposed theoretical framework presented by Varma et al. [27] enables the estimation of the level of sustainability of forest management and the monitoring of land use strategies using spatial information such as forest type, age, health, protection status, soil and water protection status, and socio-economic functions. The authors demonstrate — in a theoretical manner — the capacity of the DST to handle various types of data sources and model their related uncertainty to facilitate decision making in forest management applications.

### *1.3. Sources of information*

Topographic parameters are known to drive the spatial distribution of tree species. Statistics from Zoladeski [28] show that deciduous stands tend to grow on better drained sites in comparison to conifer stands. Wilson and Gallant [29] indicate that terrain aspect influences local solar insolation and evapotranspiration, with slope playing a role related to soil water content. Bonnan and Shugart [30] report that low solar elevation angles at high latitudes accentuate the influence of topographic aspect and slope. South facing slopes receive more solar radiation compared to north-facing slopes and as a consequence, tend to be warmer and drier. Soil moisture has been reported as the most important parameter affecting white spruce growth and productivity [31], [32]. Kenkel [33] indicates that in the boreal forests of Manitoba, Canada, trembling aspen stands can be found on well drained sites. In the sub-boreal spruce zone of British Columbia, Canada, lodgepole pine site quality improves as the soil moisture regime changes from very dry to moister, and then declines for increasingly wetter sites [34, [35].

Fire disturbance has been identified as a major factor controlling vegetation patterns (structure and composition) in boreal forests [36]. Wildfire is also known to perform an important role in the development of black and white spruce, as well as mixed spruce hardwood forests [37], [38]. More particularly, the study by Johnstone et al. [36] supports previous works indicating that the majority of tree establishment occurs within three to seven years after a forest fire in boreal forests. In addition, the authors indicate that forest patterns two or three decades after a fire disturbance can be reliably predicted from observed stand density and composition within five years after fire. Bonnan and Shugart [30] show pre-burn vegetation as a driving parameter for post-fire vegetation establishment, with different tree species having different reproduction strategies, such as wind dispersed propagules for white birch, fire resistant cones for black spruce, fire tolerant thick bark for Scots pine (*Pinus sylvestris*), and vegetative reproduction for white birch.

Despite the complexity in extracting information from VHSR imagery [2], Wulder [39] observes that VHSR images enable the characterization of individual trees, potentially leading to better forest inventory attribute estimates. Mora et al. [6] has developed a classification method to identify leading stand species with a series of tree crown metrics derived from panchromatic QuickBird imagery. Crown shapes can be predictable as each species tends to grow in an expected manner in given environmental conditions [40]. Therefore based on the species-specific tree crown characteristics described by Sayn-Wittgenstein [41] and Murtha and Sharma [42] for the species found over the study area, a series of crown object metrics were selected. Statistical tests showed significant differences between the species according to the selected metrics [6]. Utilizing crown objects to create metrics that are representative at the stand level reduces a reliance on the particular characteristics of a given crown but considers the assemblage of characteristics present. That is, crown characteristics are summarized at the stand level enabling the statistical description of conditions, including means and percentiles of crown sizes or shapes generated from the VHSR imagery. In this current study we consider these stand-level crown object metrics to build species-specific mass functions.

Landsat data is known to provide imagery with spatial and spectral characteristics uniquely suited to the development of land cover maps [43]. An example of cover type mapping over a large area is the Earth Observation for Sustainable Development of Forests or EOSD project [4], where a Landsat TM/ETM+ -based map of Canada's forests

provided broad forest classes (e.g., conifer, deciduous, mixedwood) accompanied with density sub-classes (dense, open, sparse). Less common is the development of species level information from Landsat. The capacity to spectrally distinguish between species can be problematic, often requiring ancillary data or alternate classification approaches [44]. Franco-Lopez et al. [45] and Franklin [46] used Landsat TM imagery to map forested areas with more detailed class stratification (e.g., balsam poplar, white spruce) in Minnesota, USA, and in Alberta, Canada, respectively. For additional examples, Franklin and Wulder [47] provide a review on wide area land cover classification with instruments such as Landsat.

## 2. Material and methods

### *2.1. Study area*

The study region was located in the southern Yukon Territory where four study sites were selected according to road access, the range of species and structural conditions represented, as well as availability of cloud-free QuickBird imagery (figure 1). All of the study sites had areas varying from 625 to 2400 ha and were located in the Boreal Cordillera Ecozone [48]. This Ecozone is characterized by mean annual temperatures ranging between 1°C and 5.5°C, over a typical mean range from -23°C in the winter to 11.5°C in the summer. Mean annual precipitations range from less than 300 mm in valleys shadowed by coastal mountain ranges, to more than 1500 mm at higher elevations. The topography of the Boreal Cordillera Ecozone includes extensive plateaus, mountains, wide valleys, and lowlands. The original topography in the area was altered by glaciation, erosion, solifluction, eolian, and volcanic ash deposition. The most common surface materials are glacial drift, colluvium, and outcrops. Permafrost is frequent in the more northern areas of the ecozone. Depending on local conditions, the dominant species across the four sites were black spruce (*Picea mariana*), white spruce (*Picea glauca*), lodgepole pine (*Pinus contorta*), white birch (*Betula papyrifera*), trembling aspen (*Populus tremuloides*), and balsam poplar (*Populus balsamifera*).

<< Figure 1 about here>>

### *2.2. Data*

#### *2.2.1. QuickBird imagery*

For each study site, an 8 km by 8 km panchromatic (0.45–0.90 µm) QuickBird image with a spatial resolution of 0.60 m was acquired (Table 1). Top-of-atmosphere radiance conversion was implemented according to Krause [49]. The orthorectification process (RMSE < 5 m) was undertaken as indicated in Wulder et al. [50].

<< Table 1 about here>>

#### *2.2.2. Landsat imagery*

For each study site, a co-located orthorecitfied Landsat-5 TM image was acquired from the United States Geological Survey, with scene information listed in Table 2. Further processing of the Landsat-5 TM images included a top-of-atmosphere reflectance conversion following Han et al. [51]. Image selection was based upon minimizing cloud

cover and to match, as possible, the acquisition date with that of the QuickBird imagery. Landsat TM images consist of six optical channels at a spatial resolution of 30 m.

<< Table 2 about here>>

*2.2.3. Topographic parameters*

Beven and Kirby [52] and Moore et al. [53] proposed the Topographic Wetness Index (TWI), noted $\omega$ in Eq. 1, to model the topographic control on soil moisture:

$$\omega = \ln\left(\frac{A_s}{\tan\beta}\right), \tag{1}$$

where $A_s$ is the specific catchment area and ß is the slope angle in degrees. Franklin et al. [54] have used among other parameters, the TWI to predict spatial pattern of vegetation communities.

For the four study sites, Digital Elevation Models (DEMs) were collected from the Advanced Thermal Emission and Reflection Radiometer (ASTER) database [55]. The spatial resolution is 15 m in the horizontal plane. Depending on the study site, the vertical resolution is either 11 m or 21 m. The local aspect, slope [56], and topographic wetness index (TWI) [57] were derived from the downloaded DEM tiles. Note that we did not consider elevation as a variable due to the low variation of this parameter over the study sites. In addition, soil and air temperatures are known to be important parameters influencing vegetation patterns [30]. No accurate temperature records were available for the study sites.

*2.2.4. Fire history*

The fire history map produced and maintained by the Yukon government provides spatial fire extents plus the year of fire occurrence and is suitable for use at landscape level scales [58]. Information on site 1 is suitable for studies at a scale of 1:500,000 or smaller as the information is derived from Landsat TM-5 imagery, information on site 2 is derived from a sketch map with an unspecified scale. No fire information is reported for sites 3 and 4. The temporal scale of the coverage goes back to late 1940s; however, as the Yukon-wide fire detection program was not fully operational before the 1960s, some fires in the 1940s and 1950s may not be recorded or be poorly mapped. Some stands in sites 1 and 2 were affected by fire in 2004 and 1950, respectively. In this study, only stands with a burned surface equal or greater than 75% were considered as burned.

*2.3. Classification tree*

Mora et al. [6] established a method using the spatial characteristics of within-stand objects (crowns and tree clusters) as input data for classification trees to identify stand leading species. The model was developed and applied over the same forest stands used in this study, and was calibrated with stand-level tree crown metrics derived from panchromatic QuickBird imagery. The first step of the method consisted in using an image segmentation procedure applied to the QuickBird image to delineate segments (stands) with homogeneous forest conditions, i.e., low within-stand spectral radiance variance [59], [60]. Second, individual tree crowns within these forest stands were delineated based on the spectral information from the QuickBird imagery (figure 2). The

method is based on a valley-following principle that requires lower and upper threshold values indicating whether a pixel should belong to a portion of a crown or the surrounding understory [[61]. Third, stand leading species were photo interpreted, and then a series of statistics (variance, mean, 25th, 50th, and 75th percentiles) describing crown metrics (area, perimeter, roundness) were computed at the stand level based on the crown objects. Length is defined as the square root of the object area times the length-width ratio derived from a bounding box, while roundness is defined as the difference between the radii of enclosed and enclosing ellipses of a given object [[62]. Finally, using stand random selection for initiation, a series of classification trees were established based on the crown metrics calculated at the stand level. The majority class for each stand was selected over the iterations of the multiple random selection procedure established to remove the bias that would have resulted from the use of single calibration and validation datasets.

To enable comparison between the previous [6] and current study, we reapplied the classification trees considering not only the crown metrics at the stand level derived from the QuickBird imagery, but also the information derived from Landsat TM imagery, topographic parameters, and fire history records of the area generalized at the stand level. To avoid using intercorrelated input data while still enabling vegetation characterization, we selected a limited number of spectral bands of the Landsat TM imagery. We followed the recommendations of Benson and De Gloria [63], and Horler and Ahern [64] with the selection of bands 3 (red), 4 (near-infrared), and 5 (mid-infrared). As for each of the selected Landsat TM spectral bands, the slope, aspect and TWI values were summarized at the stand level via mean values.

<< Figure 2 about here>>

*2.4. Dempster-Shafer theory*

*2.4.1. Theoretical basis of the DST*

First, one defines the frame of discernment Θ, that includes all of the $\theta_i$ states under consideration, i.e., the classes of the stratification (Eq. 2). The $\theta_i$ singleton hypotheses are meant to be exhaustive and exclusive.

$$\Theta = \{\theta_1, \theta_i, \ldots \theta_N\}, \tag{2}$$

Then, a power set $2^{\Theta}$ is derived from $\Theta$. For example, for $N$=4, the power set includes all of the subsets of Θ, and the empty set Ø, as in Eq. 3. The union class of the hypotheses $\theta_i$ and $\theta_j$ is noted ($\theta_i \cup \theta_j$).

$$2^{\Theta} = \{\theta_1, \theta_2, \theta_3, \theta_4, \theta_1 \cup \theta_2, \theta_1 \cup \theta_3, \theta_1 \cup \theta_4, \theta_2 \cup \theta_3, \theta_2 \cup \theta_4, \theta_3 \cup \theta_4, \varnothing\}. \tag{3}$$

Mass functions describing the confidence given to each focal element (i.e., each element of the power set with a non null mass) for each state of each source will be defined to allow Dempster's combination rule to fuse information sources. For a frame of discernment $\Theta$, the mass functions m(.) of each hypothesis of the power set $2^{\Theta}$ will satisfy the following requirements, for a given source:

$$\sum_{A \in 2^{\Theta}} m(A) = 1,$$
$$\text{m: } 2^{\Theta} \rightarrow [0,1], \tag{4}$$
$$\text{m } (\emptyset)=0.$$

Then, the combination rule (Eq. 5) combines the sources two by two. For $S$ sources to combine, with $S$ >2, the result of the first combination will be combined to another source, and so on until all sources are combined. Let two belief masses $m_1(.)$ and $m_2(.)$ characterize two distinct sources, then the combination rule is written as m(Ø) = 0 and $\forall\, C \in 2^{\Theta} \setminus \{\emptyset\}$:

$$m(C) \equiv [m_1 \oplus m_2](C) = \frac{\sum_{A \cap B = C} m_1(A) m_2(B)}{1 - \sum_{A \cap B = \phi} m_1(A) m_2(B)}. \tag{5}$$

The conflict between the sources, also named $k$ in the literature, is represented by the second term of the denominator in Eq. 5. Conflict equals one if the sources are completely contradictory; in such cases, fusion is not possible.

*2.4.2. Decision rules*

The most common decision rules used in the literature were defined by Shafer [1]. For $A \subseteq \Theta$, the belief (credibility) and plausibility functions are expressed as follows, respectively:

$$Bel(A) = \sum_{B \in 2^{\Theta}, B \subseteq A} m(B), \tag{6}$$

$$Pl(A) = \sum_{B \in 2^{\Theta}, A \cap B \neq \phi} m(B). \tag{7}$$

The belief of hypothesis $A$ is based upon the sum of the mass products $B$ strictly supporting the hypothesis $A$ while the plausibility function considers the mass products $B$ intersecting the hypothesis $A$. As a result the first decision rule can be considered as cautious and the second as optimistic [65].

*2.5. Mass function establishment*

The design of the mass functions was realized based on data summarized at the stand level following the polygon decomposition principle [66]. Six tree species have been found as stand leading species within the four study sites. However, two of them (white birch and balsam poplar) were discarded from the classification procedure, as their frequencies were not sufficiently high. In this study, 31 black spruce, 163 white spruce, 26 lodgepole pine, and 44 trembling aspen stands were considered. As a result, the frame of discernment of this study is defined as follows:

$$\Theta = \{Black\ spruce, White\ spruce, Lodgepole\ pine, Trembling\ aspen\},$$

*QuickBird imagery*

The mass functions for the QuickBird-derived tree crown object stand-level metrics were built with the results from the classification tree procedure established in Mora et al. [7]

and summarized in section 2.3. For each class of $\Theta$ and each stand, the mass functions resulted in the mean of the output probabilities computed for each stand over the iterations of the multiple random selection procedure. Then masses for the union classes were calculated based on the following rules:

$$\text{if } |\Delta_{m(\theta i), m(\theta j)}| > 0, \text{ then } m(\theta_i \cup \theta_j) = -|\Delta_{m(\theta i), m(\theta j)}| + 1, \quad (8)$$

$$\text{if } \Delta_{m(\theta i), m(\theta j)} = 0,\ m(\theta_i), m(\theta_j) > 0, \text{ then } m(\theta_i \cup \theta_j) = m(\theta_i) = m(\theta_j), \quad (9)$$

$$\text{if } \Delta_{m(\theta i), m(\theta j)} = 0,\ m(\theta_i) = m(\theta_j) = 0, \text{ then } m(\theta_i \cup \theta_j) = 0, \quad (10)$$

with $\Delta_{m(\theta i), m(\theta j)}$ being the difference between the mass values of the singleton hypotheses forming the union class ($\theta_i \cup \theta_j$). Eq. 8 was designed so that the smaller $|\Delta_{m(\theta i), m(\theta j)}|$ was, i.e., both singleton hypotheses were increasingly equally probable, the greater the mass allocation to ($\theta_i \cup \theta_j$) was, and conversely (figure 3). Once all mass functions were calculated, a normalization to unity (i.e., 1) was performed to comply with Eq. 4. Eq. 9 considers the case masses m(θi) and m(θj) are equal and non-null while Eq. 10 considers the case masses m(θi) and m(θj) are both null.

<< Figure 3 about here>>

*Landsat TM imagery*

Mass functions for the Landsat TM imagery were designed considering bands 3, 4, and 5 only, so that the results were comparable with those from the classification tree. For each band, the stand-level mean reflectance values were computed based on the pixels located within the boundaries of each stand. The Fuzzy Statistical Expectation Maximization (FSEM) method, a supervised classification algorithm proposed by Germain *et al*. [67], was used to estimate the mass functions. The FSEM has the ability to produce union classes from the original input singleton classes. This multi-iterative algorithm computes posterior probabilities and can be either stopped after a number of iterations have been reached or after the class attribution turn-over between iteration *n* and *n*-1 gets below a given percentage. In this study the percentage was empirically fixed at 1%, i.e., the minimal and most conservative threshold value. For each class, two-thirds of the forest stands were randomly selected and used as a calibration dataset. Twenty stands were selected at random with calibrations of the FSEM then performed. Following selection and calibration, for each class and each stand, the mean of the twenty posterior probabilities were calculated and used as mass functions for the Landsat TM imagery.

*Topographic parameters*

For each topographic parameter, the mean stand value of the source was computed at the stand level. Then mass functions for the terrain aspect (figure 4), the slope (figure 5) and the TWI, were designed based on literature cited in section 2.2.3. The highest mass value, empirically fixed at a value of 0.8, was attributed to the mean slope value found in the statistics from Zoladeski [28]. A value of 0.8 was chosen as we considered the maximum mass value should not be too high to consider the intertwined effects of the biophysical factors influencing the species patterns and the resulting uncertainty and vagueness inherent to the studies our work was based on. A value of 0.8 was also chosen as a maximum mass value for the other sources. The minimum and maximum values correspond to lowest and highest slope values found in the same reference (Table 3). For

the TWI, the mass functions of the black spruce (Eq. 11) and trembling aspen (Eq. 12) were designed based on the study from Mackey et al. [67]. The reference provided scatter plots of the observed probabilities for the two species as a function of the topographic wetness index. Mass functions were bell-shaped on the domain of interest and were obtained applying regressions on points derived from the graphs. As no precise information was found for lodgepole pine and white spruce, bell-shaped distributions were assumed for these species as well. The Gaussian distribution model was chosen to represent the functions, with means of 10 and 6 for the white spruce and the lodgepole pine, respectively. These mean values were selected relative to those found for the two other species and according to soil moisture preferences [28]. A standard deviation of 1 was chosen to get a standardized-normal curve [69]. Finally, for each of these three sources, mass functions for the union classes were based on Eq. 8.

$$y = 0.36 + 0.47 * \cos(0.19 * x - 2.4), \quad (11)$$

$$y = -0.12 + 0.3 * x - 0.003 * x^2 + 0.0009 * x^3, \quad (12)$$

with $x$: the TWI value, and $y$: the corresponding mass value.

<< Figure 4 about here>>
<< Figure 5 about here>>
<< Table 3 about here>>

*Fire history map*

Attribution of mass values for each species was based on the nature of the species of the adjacent remaining stands. For site 1, partially burned in 2004, 80% of adjacent stands had trembling aspen as leading species and 20% had white spruce. For site 2, partially burned in 1950, 60% of adjacent stands had white spruce as leading species and 40% had black spruce. The mass values for each species were assigned according to the relative abundance of the species surrounding each stand as specified in Table 4. We empirically fixed the highest mass value at 0.8. On both sites, mass functions for the union classes were based on Eq. 8. Stands in sites 3 and 4 and those from sites 1 and 2 with a burned area lower than 75%, were assigned a mass value of 0 for this source.

<< Table 4 about here>>

*2.6. Source combination tests*

We tested a series of source combinations starting with the fusion of the QuickBird source with one other source (Landsat TM imagery, slope, aspect, TWI, or the fire history map). Then we applied the DST on every possible three, four, and five-source combinations. The six sources were finally combined. The maximum credibility and the maximum plausibility were both tested as decision rules after the source combination. To assess the performance of the combination, the overall accuracy as well as the class accuracies were systematically compared with those obtained using the classification tree-based method.

## 3. Results

*3.1. Spectral class separability*

The Landsat TM spectral class separability of the species considered in this study was tested to characterize the capacity of the selected Landsat bands to provide discriminant information on the species. The transformed divergence method [68] was used knowing that a perfect separability equals two (Table 5). Trembling aspen, the representative unique deciduous species of the study, has a high level of separability with black spruce and lodgepole pine. However, its separability with white spruce is low. White spruce stands have a low separability with black spruce stands as well, but have a high separability with lodgepole pine stands. Black spruce stands have a high separability with lodgepole pine stands.

<< Table 5 about here>>

*3.2. Classification tree method*

The method based on classification trees provided an overall accuracy of 67.3%. The error matrix displayed in Table 6 shows class accuracies ranging from 40.7% for the white spruce stands to 100% for the black spruce stands. Table 7 provides the proportions of metrics selected across the iterations. Crown metrics and to a lesser extent Landsat-based metrics, were the most frequently selected statistics, while the topographical and fire history record statistics were scarcely or never selected.

<< Table 6 about here>>
<< Table 7 about here>>

*3.3. Fusion with the DST combination rule*

Tables 8 and 9 present the accuracies obtained when fusing the QuickBird source with one other source, considering the maximum credibility and plausibility, respectively. Results obtained with the maximum plausibility are presented as an example in Table 9 only, as the maximum plausibility systematically provided worse overall accuracies than the maximum credibility; whatever the combination and the number of sources involved. Table 10 provides the accuracies resulting from the fusion of the Landsat TM image and one other source. Table 11 summarizes the best results produced over all the possible *n*-source combinations with $n \geq 3$. The best overall accuracy (70.4%) was obtained with the fusion of the QuickBird and the Landsat TM sources. The addition of the aspect to the previous combination provided equivalent results. This three-source combination resulted in small class-accuracy changes only. Combinations with four or more sources provided lower overall accuracies.

<< Table 8 about here>>
<< Table 9 about here>>
<< Table 10 about here>>
<< Table 11 about here>>

## 4. Discussion

*4.1. Classification trees*

The classification-tree based method provided an overall accuracy of 67.3% with varying class accuracies (Table 6). As for the classification-tree based method applied on a series of metrics derived from panchromatic QuickBird imagery only [6], the accuracy with which white spruce stands were identified did not reach a satisfactory level (40.7%). As a climax species, white spruce is widespread in north-western Canada and often co-dominates stands with other tree species [71]. In addition, white spruce grows on a wide variety of soil conditions [72]. The simultaneity of these ecological traits can be responsible for the increased variance of the crown metrics observed for this species [6]. The number of white spruce stands used for this analysis was much larger than the number of stands used for the other species, thereby broadening the range of environmental conditions present in white spruce stands relative to stands with other leading species and reflecting the higher tolerance which white spruce has for variability in soil moisture regimes compared to black spruce, for example. Overall, sources of crown shape alterations can also be due to side shade effect, possible phototropism, climatic events such as wind and ice storms, and sudden changes in the tree's hormonal balance [40].

Table 7 shows that tree crown and Landsat band metrics were the most commonly selected inputs for the classification trees. Mean TWI and aspect were rarely selected (< 2%) and slope and fire history were never selected, suggesting that the non-satellite data sources were not sufficiently informative in comparison to the remotely sensed imagery. The nature of the non-satellite data sets may play a role, for instance in the case of the fire maps, which are binary and which may only be suitable for use at scales of 1:250,000 or smaller [58]. Burned area products are of a more generalized nature when compared to the other available, higher spatial resolution data sources. Further, burned area depictions can also include unburnt islands and differing levels of burn intensity, thereby representing a range of conditions not captured by the binary product. Furthermore, as shown in the literature review, Landsat imagery has not been used extensively to discriminate stand species over boreal environments, but rather to distinguish cover types or broad forest classes (e.g., coniferous, deciduous, mixed). The spectral and spatial characteristics of Landsat data, combined with the spectral similarities found for species (which is further exacerbated by the averaging of reflectance over a larger pixel), does not favour the use of Landsat as a stand-alone data source for species classification in complex environments. Compared to the study of Mora et al. [6], the addition of more input data sources decreased the overall accuracy by 5%. The metrics that were most commonly selected over the iterations remained similar to those in Mora et al. [6] with the inclusion of mean stand reflectance values from the near- and middle-infrared bands (bands 4 and 5) of the Landsat TM imagery. Bands 4 and 5 were selected for 24.6% and 44.1% of iterations, respectively (Table 7) indicating a utility and notable explanatory power in these inputs.

Comparing these results with those obtained in Mora et al. [6], the addition of Landsat TM imagery may have introduced confusion between the classes, supporting the possible use of Landsat data as a pre-classification stratification layer rather than as a variable in the classifier. The infrequency with which the other ancillary data sources were selected for the classification trees suggests that these data may be of insufficient quality or spatial resolution for modelling as drivers of species patterns. The mixture of spatial resolutions (scales) of the input data sources likely also played a role, with the

most detailed variables from the VHSR imagery also providing the most explanatory power for species discrimination. The scale of the VSHR data provides the closest match to the actual species information of interest, where differentiation is present at the crown level and captured through the image spatial structure of crown metrics, rather than through more generalized spectral (Landsat imagery) or spatial characteristics (terrain metrics).

*4.2. Data fusion*

For the fusion process, the maximum credibility decision rule was more efficient to identify the leading species than the maximum plausibility (Tables 8 and 9). The trend was systematically observed, whatever the source combination. As presented in section 4.2.2., the maximum credibility was a more cautious rule as it considers information strictly supporting a hypothesis.

Two source combinations (Landsat TM and QuickBird imagery; Landsat TM and QuickBird imagery plus aspect) provided the best overall accuracy (70.4%) with similar class-accuracies (Tables 8 and 11). These source combinations improved the overall accuracy by 3.1% compared to the conventional classification-tree based method (from 67.3% to 70.4%). For both cases, class accuracies remained unbalanced as the white spruce stands remained poorly identified (26.5% and 24%). The mass functions of the QuickBird imagery were derived from the study of Mora et al. [6]. Class confusion insights from this original study were transferred to the current DST-based model, and now partially explain the obtained accuracies. Furthermore, stand leading-species were identified from the photo-interpretation of the QuickBird imagery. Consequently, some misidentifications may have occurred, broadening the range of crown metrics and reflectance values from Landsat TM imagery, respectively.

The addition of the aspect or the fire record map to the QuickBird imagery provided similar results to those obtained when replacing the QuickBird imagery by the Landsat TM imagery (Tables 8 and 10). For the Landsat TM imagery, the FSEM was able to design mass functions enabling a better consideration of the information of the satellite imagery, compared to the classification tree-based model. The “fuzziness” of the masses computed by the FSEM in conjunction with the combination rule of the DST demonstrated an improved capacity to extract information from the Landsat imagery compared to the classification tree algorithm principle that does not follow a probability model [8]. The fusion of the slope or the TWI sources to the Landsat TM provided better results than those involving the QuickBird imagery. The combinations with four, five, and six sources did not improve the accuracies. However, some combinations provided accuracies similar to the highest accuracies obtained with two or three sources only (Table 11). Such results can be explained by the complementary and non-contradictory information provided by the fused sources that resulted in a low conflict rate $k$ (Eq. 5) that ranged from 0.15 to 0.35. As for the two and three ancillary source combinations, it can be noted that for the best four and five source combinations, Landsat TM, QuickBird, and aspect sources were involved in the fusion. It appears that these three sources provided complementary information: QuickBird imagery provided structural information through the stand-level crown metrics; Landsat TM imagery provided more detailed information in the visible and near-infrared spectral range; and aspect provided more meaningful and complementary information on species spatial patterns compared to

the other ancillary sources. The other sources associated to their mass functions did not provide information that could be informatively used by the fusion process. As these sources were already not selected by the classification tree, one can predict that the manner in which the mass functions were established is not the main driver of the observed decreases of the accuracies. Instead, these results reinforce the hypothesis that the data available was not appropriate (due to considerations of scale, attribute accuracy, among other possible issues) to enable the capture of the local ecological processes necessary for an improved classification capacity. Despite the theoretical underpinnings of the TWI for modelling the topographic impacts on soil moisture, Mackey et al. [67] indicate that this index assumes steady-state conditions and spatially invariant conditions for both transmissivity and infiltration, as well as the absence of complex or deep subsurface drainage, so that subsurface flows follow surface morphology. The fire record map standards from 1997 originally limited the polygon size to 200 ha. Current standards allow for polygons as small as 0.2 ha. Some fires in the 1940s and 1950s were not recorded or poorly mapped as access to regular aerial mapping was not readily available during this historic period. Furthermore, as previously mentioned, burned areas were broadly delineated and did not account for islands of unburned forest within the fire boundary [58].

Overall, the fusion did not markedly outperform the results obtained by Mora et al. [6]. The authors of the aforementioned study obtained an overall accuracy of 72.5%, and with a limited class-accuracy for white spruce stand as well (43.9%). In the current study, the fusion of the QuickBird imagery and aspect provided a similar class-accuracy (43.2%) for white spruce stands. This combination had a lower overall accuracy (69.4%) but provided a markedly lower class-accuracy standard-deviation (23.5 percentage points (pp)) compared to the one obtained with the fusion of the QuickBird and Landsat TM imagery (31.2 pp). As stated in section 1.3, the influence of aspect can be increased under northern latitudes where low solar elevation angles occur. This phenomenon can partially explain why this parameter appeared as a complementary source of information to the QuickBird imagery. The improvement of the overall accuracy by the DST method compared to the classification tree demonstrates the power of the DST for incorporating different data sources. It also indicates the limitations imposed by the characteristics of the input data (e.g., scale, range of measures, etc.) that may be partially mitigated by the design of the mass functions.

*4.3. Future work*

Potential avenues could be explored to improve the class accuracies. Training data with known consistency and an appropriate scale could be designed with sample plots established across the full range of conditions (topography and disturbance history) encountered over the study area. The extent of the road network in Canada's north restricts access to forest stands. However, the double sampling technique developed by the United States Department of Agriculture - Forest Service [73] could be employed to facilitate plot establishment while reducing fieldwork and associated costs, as shown by Wulder et al. [74]. In addition, we recommend the use of VHSR imagery acquired with similar acquisition parameters (date and off nadir view angle notably) to build a specific model as varying conditions can alter the homogeneity of the crown objects and their derived metrics. Note that in our study Site 3 had a significantly different satellite

azimuth (Table 1). Acquisition of optical imagery with cloud-free conditions in northern latitudes is an issue and explains in part why the acquisition parameters of the four images varied.

Research efforts could focus on the improvement of the design of mass functions. These functions were empirically established as per other studies using the DST [74], [25], [75]. The knowledge-driven establishment of the functions could be updated according to new knowledge on species ecology. In addition, other mass design frameworks like the discounting framework [1], could be implemented to allow alternative mass assignments. It is important to note that mass functions should be designed specifically for areas with similar biophysical characteristics and equivalent species composition. In our study, the four study sites were in a homogenous region and had similar environmental and physical characteristics. Finally, the data and the associated mass functions used in this study do not justify the use of other combination rules such as those proposed in Smarandache and Dezert [18], as low conflict rates were found. Considering the quality of the non-satellite data sources used in this study, we recommend that—based upon the methods and rules that we applied—leading stand species characterization over boreal forests can be reliably and parsimoniously undertaken using only the panchromatic QuickBird imagery, with the classification-tree based method similar to that developed by Mora et al. [6].

## 5. Conclusion

The highest overall accuracy for leading species identification (70.4%) was obtained through fusion of the QuickBird and Landsat TM imagery, improving on the result obtained using the classification tree method by 3.1%. The addition of aspect as a third ancillary data source led to an equivalent overall accuracy, but with modified individual class accuracies for white spruce and trembling aspen. Despite the proven capacities of the DST to improve classification accuracy compared to classical methods, the DST in this case did not outperform the results obtained with a classification-tree based method applied on metrics derived from a single source of information (panchromatic QuickBird imagery), as shown in a previous study. However, the current study demonstrated how a data fusion process could be implemented to map leading stand species in a boreal environment. Furthermore, the study demonstrated the critical aspect of data input quality to successfully enable the classification process, and the limitations of the classification trees compared to the DST when an equivalent input dataset is used. Finally, our discussion highlighted the necessity to capture and relate knowledge of the ecological processes taking place in boreal forested environments for improved specification of the mass functions. DST can be implemented following the examples provided in Smarandache and Dezert [18]. In addition, DST is increasingly available through software tools such as MATLAB® and IDRISI®.

## 6. Outlook

Forest inventories are often driven by information interpreted from air photos, including national inventories. VHSR imagery offers a satellite-based source of information analogous to air photographs. Sample based national inventory programs, such as Canada's National Forest Inventory (NFI) is based upon 2 x 2 km photo plots (samples) located on a 20 x 20 km national grid. Collection, delineation, interpretation, attribution,

update, and management of approximately 20,000 photo plots is required to implement the NFI. The use of VHSR imagery offers opportunities for flexibility in data acquisition and automation of delineation (through segmentation) and attribution (through image processing) activities.

When compared to the results of Mora et al. [6] the current study produced a 5% lower overall accuracy for the classification tree-based method and 2.1% lower for the best DST fusion result. These results relate the importance of the quality of the data and the necessity to provide complementary input data sources to establish meaningful additional information for the classification algorithm. Considering the best fusion classification result, the lesson for an operational program requiring detailed stand level information is that the more parsimonious panchromatic image processing approach from Mora et al. [6] may be applied.

**Acknowledgments**

This research was enabled through funding of "EcoMonitor: Northern ecosystem climate change monitoring" through the Government Related Initiatives Program (GRIP) of the Canadian Space Agency. Additional funding and support was also provided by the Canadian Forest Service (Natural Resources Canada), including the National Forest Inventory Project Office.

**References**

[1] P. Boudewyn, X. Song, S. Magnussen, M.D. Gillis, Model-based, volume-to-biomass conversion for forested and vegetated land in Canada, Canadian Forest Service, Pacific Forestry Centre, BC-X-411, Victoria, British Columbia, 2007.

[2] M.J. Falkowski, M.A. Wulder, J.C. White, M.D. Gillis, Supporting large-area, sample-based forest inventories with very high spatial resolution satellite imagery, Prog. in Phys. Geography 33 (2009) 403−423.

[3] Natural Resources Canada, The state of Canada's forests - Annual report, Canadian Forest Service, Ottawa, Ontario, 2010.

[4] M.A. Wulder, J.C. White, M. Cranny, R. J. Hall, J. E. Luther, A. Beaudoin, D.G. Goodenough, J.A. Dechka, Monitoring Canada's forests. Part 1: Completion of the EOSD Land Cover Project, Can. J. of Remote Sens. 34 (2008a) 549−562.

[5] NFI, 2006. https://nfi.nfis.org/index.php [last accessed on April 30, 2012]

[6] B. Mora, M.A. Wulder, J.C. White, Identifying leading species using tree crown metrics derived from very high spatial resolution imagery in a boreal forest environment, Can. J. of Remote Sens. 36 (2010a) 332-344.

[7] B. Mora, M.A. Wulder, J.C. White, Segment-constrained regression tree estimation of forest stand height from very high spatial resolution panchromatic imagery over a boreal environment, Remote Sens. of Envir. 114 (2010b) 2474-2484.

[8] L. Breiman, J.H. Friedman, R.A. Olshen, C.J. Stone, Classification and regression trees, Chapman and Hall/CRC, Boca Raton, Florida, 1998.

[9] A.P. Dempster, A generalization of Bayesian inference, J. of the Royal Stat. Soc. Series B 30 (1968) 205-247.

[10] G. Shafer, A Mathematical Theory of Evidence, Princeton Univ. Press, Princeton, New Jersey, 1976.

[11] G.G. Moisen, T.S. Frescino, Comparing five modelling techniques for predicting forest characteristics, Ecol. Modell. 157 (2002) 209-225.
[12] G.G. Moisen, E.A. Freeman, J.A. Blackard, T.S. Frescino, N.E. Zimmermann, T.C. Edwards Jr., Predicting tree species presence and basal area in Utah: A comparison of stochastic gradient boosting, generalized additive models, and tree-based methods, Ecol. Modell. 199 (2006) 176-187.
[13] W. Aertsen, V. Kint, J.V. Orshoven, K. Özkan, B. Muys, Comparison and ranking of different modelling techniques for prediction of site index in Mediterranean mountain forests, Ecol. Modell. 221 (2010) 1119-1130.
[14] J. Elith, J.R. Leathwick, T. Hastie, A working guide to boosted regression trees, J. of Anim. Ecol. 77 (2008) 802–813.
[15] M. Egmont-Petersen, D. De Ridder, H. Handels, Image processing with neural networks - a review, Pattern Recognit. 35 (2002) 2279–2301.
[16] T. Bayes, An Essay towards solving a Problem in the Doctrine of Chances. By the late Rev. Mr. Bayes, communicated by Mr. Price, in a letter to John Canton, M. A. and F. R. S., Philosophical Transactions of the Royal Society of London 53 (1763) 370–418.
[17] L.A. Zadeh, Fuzzy sets, Inf. Control 8 (1965) 338-353.
[18] F. Smarandache, J. Dezert, Advances and applications of DSmT for information fusion (Collected works), Vol. 2, Smarandache, F. and Dezert, J. (Ed.), American Research Press, Rehoboth, New Mexico, 2006.
[19] L.A. Zadeh, A simple view of the Dempster-Shafer theory of evidence and its implication for the rule of combination, AI Mag. 7 (1986) 85-90.
[20] L.A. Zadeh, Fuzzy Sets as the Basis for a Theory of Possibility, Fuzzy Sets and Syst. 1 (1978) 3-28.
[21] D. Dubois, H. Prade, Representation and combination of uncertainty with belief functions and possibility measures, Computational Intelligence 3 (1988) 244-264.
[22] P. Smets, The combination of evidence in the transferable belief model, IEEE Transactions on Pattern Analysis and Machine Intell. 12 (1990) 447-458.
[23] F. Smarandache, J. Dezert, (Eds.) Advances and Applications of DSmT for Information Fusion (Collected works), American Research Press, Rehoboth, New Mexico, 2004.
[24] B. Mora, R.A. Fournier, S. Foucher, Application of Evidential Reasoning to Improve Regenerating Forest stand Mapping, Int. J. of Appl. Earth Observation and Geoinformation 13 (2010c) 458-467.
[25] L. Cayuela, J.D. Golicher, J. Salas Rey, J.M. Rey Benayas, Classification of a complex landscape using Dempster-Shafer theory of evidence, Int. J. of Remote Sens. 27 (2006) 1951-1971.
[26] S.E. Franklin, D.R. Peddle, J.A. Dechka, G.B. Stenhouse, Evidential reasoning with landsat TM, DEM and GIS data for landcover classification in support of grizzly bear habitat mapping, Int. J. of Remote Sens. 23 (2002) 4633-4652.
[27] V.K. Varma, I. Ferguson, I. Wild, Decision support system for the sustainable forest management, Forest Ecol. and Manage. 128 (2000) 49-55.
[28] C.A. Zoladeski, D.W. Cowell, Ecosystem classification for the Southeast Yukon: field guide, first approximation. Yukon Renewable Resources, Whitehorse, Yukon, 1996.

[29] J.P. Wilson, J.C. Gallant, Terrain analysis, Principles and Applications, John Wiley and Sons, New York, 2000.
[30] G.B. Bonnan, H.H. Shugart, Environmental factors and ecological processes in boreal forests, Annu. Rev. Ecol. Syst. 20 (1989) 1-28.
[31] D. L. Pluth, I.G.W. Corns, Productivity of conifers in western Canada boreal forests in relation to selected environmental factors, in: Ballard, R., & Gessel, P.G. (Eds.), IUFRO Symposium on Forest Site and Continuous Productivity, General Technical Report PNW-163, USDA, Forest Service, Pacific Northwest Forest and Range Experiment Station, Portland, Oregon, 1983, pp. 101-111.
[32] G.G. Wang, K. Klinka, Site-specific curves for white spruce (Picea glauca [Moench] Voss) stands based on stem analysis and site classification, Ann. of Forest Sci. 52 (1995) 607-618.
[33] N. Kenkel, C. Foster, R. Caners, R. Lastra, D. Walker, Spatial and temporal patterns of white spruce recruitment in two boreal mixedwood stands, Sustainable forest management network, Duck Mountains, Manitoba, 2003.
[34] G.J. Kayahara, K. Klinka, I. Moss, Influence of site quality on lodgepole pine and interior spruce site index in the sub-boreal spruce zone of British Columbia, Report to Northwood Pulp and Timber Ltd., Prince George, British Columbia, 1994.
[35] Q. Wang, G.G. Wang, K.D. Coates, K. Klinka, Use of site factors to predict lodgepole pine and interior spruce site index in the sub-boreal spruce zone, Research Note No. 114, Ministry of Forest, Victoria, British Columbia, 1994.
[36] J.L. Johnstone, F. S. Chaplin Ill, J. Foote, S. Kemmett, K. Price, L. Viereck, Decadal observations of tree regeneration following fire in boreal forests, Can. J. of Forest Res. 34 (2004) 267-273.
[37] M. J. Foote, Classification, description, and dynamics of plant communities after fire in the taiga of interior Alaska, Pacific Northwest Range and Experiment Station Research Paper PNW-307, United States Department of Agriculture Forest Service, Portland, Oregon, 1983.
[38] S.A. Drury, P.J. Grimsson, Fire history and fire management implications in the Yukon Flats National Wildlife Refuge, interior Alaska, Forest Ecol. and Manage. 256 (2008) 304-312.
[39] M.A. Wulder, Optical remote sensing techniques for the assessment of forest inventory and biophysical parameters, Prog. in Phys. Geography 22 (1998) 449−476.
[40] C.D. Oliver, B.C. Larson, Forest stand dynamics – update edition, John Wiley and Sons, New York City, New York, 1996.
[41] L. Sayn-Wittgenstein, Recognition of tree species on aerial photographs. Ottawa, Ontario, 1978.
[42] P. Murtha, R. S. Sharma, Remote Sensing, Photo Interpretation and Photogrammetry, in: Forestry Handbook for British Columbia. 5th Ed., University of British Columbia (Eds.), Vancouver, BC, 2005, pp. 657-662.
[43] M.A. Wulder, J.C. White, S.N. Goward, J.G. Masek, J.R., Irons, M. Herold, W.B. Cohen, T.R. Loveland, C.E. Woodcock, Landsat continuity: Issues and opportunities for land cover monitoring, Remote Sens. of Environ. 112 (2008b) 955-969.
[44] C.G. Homer, R.D. Ramsey, T.C. Edwards Jr., A. Falconer, Landscape Cover-Type Modelling Using a Multi-Scene Thematic Mapper Mosaic, Photogrammetric Eng. & Remote Sens. 63 (1997) 59-67.

[45] H. Franco-Lopez, A.R. Ek, M.E. Bauer, Estimation and mapping of forest stand density, volume, and cover type using the k-nearest neighbors method, Remote Sens. of Environ. 77 (2001) 251-274.
[46] S.E. Franklin, Discrimination of subalpine forest species and canopy density using digital CASI, SPOT PLA, and Landsat TM data, Photogrammetric Eng. & Remote Sens. 60 (1994) 1233-1241.
[47] S.E. Franklin, M.A. Wulder, Remote sensing methods in medium spatial resolution satellite data land cover classification of large areas, Prog. in Phys. Geography 26 (2002) 173-205.
[48] Ecological Stratification Working Group, A national ecological framework for Canada. Agriculture and Agri-Food Canada, Research Branch, Ottawa, Ontario, 1995. Available from: http://sis.agr.gc.ca/cansis/nsdb/ecostrat/intro.html [last accessed April 30, 2012].
[49] K. Krause, Radiance conversion of QuickBird data - technical note, Digital Globe, Longmont, Colorado, 2003.
[50] M.A. Wulder, E. Loubier, D. Richardson, Landsat-7 ETM+orthoimage coverage of Canada, Can. J. of Remote Sens. 28 (2002) 667−671.
[51] T. Han, M.A. Wulder, J.C. White, N.C. Coops, M.F. Alvarez, C. Butson, An efficient protocol to process Landsat images for change detection with Tasselled Cap Transformation, Geoscience and Remote Sens. Lett. 4 (2007) 147-151.
[52] K.J. Beven, M.J. Kirby, A physically-based, variable contributing area model of basin hydrology, Hydrological Sciences Bulletin 24 (1979) 43-69.
[53] I.D. Moore, R.B. Grayson, A.R. Ladson, Digital terrain modelling: a review of hydrological, geomorphological, and biological applications, Hydrological Processes 5 (1991) 3-30.
[54] J. Franklin, Terrain variables used for predictive mapping of vegetation communities in southern California, in: Terrain Analysis: Principles and Applications, J. P. Wilson and J. C. Gallant (Eds.), John Wiley and Sons Inc., New York City, New York, 2000, pp. 331–354.
[55] United States Geological Survey. (2009, June). Routine Global Digital Elevation Model. Available from: https://lpdaac.usgs.gov/content/view/full/11033. [last accessed April 30, 2012]
[56] ESRI, ArcDoc Version 9.3, Environmental Systems Research Institute, Redlands, California, 2006.
[57] P.E. Gessler, I.D. Moore, N.J. McKenzie, P. J. Ryan, Soil-landscape modelling and spatial prediction of soil attributes, Int. J. of Geographical Inf. Syst. 9 (1995) 421-432.
[58] Anonymous, Yukon Fire History Metadata, Government of the Yukon Territory Community Services, Protective Service Branch, Wildland Fire Management, Version 2008.01, White Horse, Yukon Territory, 2008.
[59] M. Baatz, M. Schäpe, Multiresolution segmentation: An optimization approach for high quality multi-scale image segmentation, in: Angewandte Geographische Informationsverarbeitung XII, Beiträge zum AGIT19 Symposium Salzburgz, Strobl, J. et al. (Eds), Herbert Wichmann Verlag, Karlsruhe, Germany, 2000, pp. 12-23.
[60] Definiens, eCognition 4 user guide, Munich, Germany, 2004.

[61] F.A. Gougeon, A crown-following approach to the automatic delineation of individual tree crowns in high spatial resolution aerial images, Can. J. of Remote Sens. 21 (1995) 274−284.
[62] Russ, J. C., The image processing handbook – 4th Ed, CRC Press Inc, Boca Raton, Florida, 2002.
[63] A. Benson, S. DeGloria, Interpretation of Landsat-4 thematic mapper and multispectral scanner data for forest surveys, Photogrammetric Eng. & Remote Sens. 51 (1985)1281-1289.
[64] D.N.H. Horler, F.J. Ahern, Forestry information content of Thematic Mapper data, Int. J. of Remote Sens. 7 (1986) 405-428.
[65] Bracker H., Utilisation de la théorie de Dempster-Shafer pour la classification d'images satellitaires à l'aide de données multi-sources et multitemporelles, Thèse de l'Université de Rennes I, Rennes, 1996.
[66] M. Wulder, S.E. Franklin, Polygon decomposition with remotely sensed data: Rationale, methods, and applications, Geomatica 55 (2001) 11-21.
[67] M. Germain, M. Voorons, J.M. Boucher, G.B. Bénié, Fuzzy statistical classification method for multiband image fusion, in: Proceedings of the 5th International Conference on Information Fusion, 8-11 July, Annapolis, USA, IEEE, Piscataway, New Jersey, 2002, 178-184.
[68] B.G. Mackey, I.C. Mullen, K.A. Baldwin, J.C. Gallant, R.A. Sims, D.W. McKenney, Towards a spatial model of boreal forest ecosystems: the role of digital terrain analysis, in: Terrain Analysis: Principles and Applications, J. P. Wilson and J. C. Gallant (Eds.), John Wiley and Sons Inc., New York City, New York, 2000, pp. 391–423.
[69] J. H. Zar, Biostatistical analysis, 5th Edition, Prentice-Hall Inc., Upper Saddle River, New Jersey, 2010.
[70] T.M. Lillesand, R.W. Kiefer, Remote sensing and image interpretation, 3rd edition, John Wiley & Sons Inc., New York, 1994.
[71] H. J. Lutz, Ecological effects of forest fires in the interior of Alaska, Tech. Bull., No. 1133, Washington, District of Columbia, 1956.
[72] F.H. Eyre, Forest cover types of the United States and Canada, Society of American Foresters, Washington, District of Columbia, 1980.
[73] USDA Forest Service, Forest service resource inventories: An overview. Forest Inventory, Economics and Recreation Research, Washington, District of Columbia, 1992.
[74] M.A. Wulder, S.M. Ortlepp, J.C. White, N.C. Coops, S.B. Coggins, Monitoring tree-level insect population dynamics with multi-scale and multi-source remote sensing, J. of Spatial Sci. 53 (2008c) 49-61.
[75] W.B. Luo, B. Caselton. Using Dempster-Shafer theory to represent climate change uncertainties, J. of Environ. Manage. 49 (1997) 73-93.
[76] M. H. Tangestani, A comparative study of Dempster-Shafer and fuzzy models for landslide susceptibility mapping using a GIS: An experience from Zagros Mountains, SW Iran, J. of Asian Earth Sci. 35 (2009) 66-73.

List of Tables

**Table 1. QuickBird image acquisition parameters.**

| | Acquisition date | Size (ha) | Plot center UTM Zone 9N | | Solar azimuth (degrees) | Solar elevation (degrees) | Satellite azimuth (degrees) | Satellite elevation (degrees) | Off-nadir view angle (degrees) | In-track view angle (degrees) | Cross-track view angle (degrees) |
|---|---|---|---|---|---|---|---|---|---|---|---|
| | | | Easting (m) | Northing (m) | | | | | | | |
| **Site 1** | 2007-08-28 | 625 | 45116 | 7133046 | 176.6 | 35.7 | 197.3 | 77.3 | 11.6 | -11.7 | -0.2 |
| **Site 2** | 2007-08-18 | 2400 | 118968 | 7030079 | 174.5 | 39.9 | 175.8 | 84.1 | 5.3 | -5.0 | 1.8 |
| **Site 3** | 2006-06-12 | 625 | 130603 | 6866945 | 171.8 | 51.4 | 57.2 | 78.5 | 10.9 | 8.1 | 7.3 |
| **Site 4** | 2007-06-08 | 1375 | 508030 | 6661737 | 172.9 | 52.8 | 173.1 | 88.3 | 1.3 | -1.3 | 0.4 |

**Table 2. Landsat TM 5 acquisition parameters.**

| | Acquisition date | Landsat WRS Path / Row | Solar azimuth (degrees) | Solar elevation (degrees) |
|---|---|---|---|---|
| **Site 1** | 2007-07-19 | P62R15 | 162.7 | 45.7 |
| **Site 2** | 2006-07-11 | P59R17 | 158.8 | 49.2 |
| **Site 3** | 2007-07-19 | P62R16 | 160.8 | 46.8 |
| **Site 4** | 2007-08-28 | P54R18 | 161.6 | 38.3 |

**Table 3. Parameters for the design of the mass functions of the singleton classes for the slope.**

| Species | Minimum (degrees) | Mean (degrees) | Maximum (degrees) |
|---|---|---|---|
| **Black spruce** | 0 | 18 | 84 |
| **White spruce** | 0 | 8 | 78 |
| **Lodgepole pine** | 0 | 10 | 40 |
| **Trembling aspen** | 0 | 23 | 89 |

**Table 4. Mass values of singleton classes for both fire dates with BS: black spruce, WS: white spruce, LP: lodgepole pine and TA: trembling aspen.**

| Fire date | Black spruce | White spruce | Lodgepole pine | Trembling aspen |
|---|---|---|---|---|
| **1950** | 0.35 | 0.45 | 0.1 | 0.1 |
| **2004** | 0.1 | 0.2 | 0.1 | 0.6 |

**Table 5. Transformed divergence between classes over the Landsat TM imagery (bands 3, 4, and 5).**

| | Black spruce | White spruce | Lodgepole pine |
|---|---|---|---|
| **White spruce** | 1.00 | | |
| **Lodgepole pine** | 1.7 | 1.5 | |
| **Trembling aspen** | 1.8 | 0.9 | 1.9 |

**Table 6. Error matrix (%) from the classification tree-based procedure.**

| | Black spruce | White spruce | Lodgepole pine | Trembling aspen |
|---|---|---|---|---|
| **Black spruce** | **100** | 0 | 0 | 0 |
| **White spruce** | 12.3 | **40.7** | 36.5 | 10.5 |
| **Lodgepole pine** | 12.5 | 12.5 | **75** | 0 |
| **Trembling aspen** | 13.9 | 11.6 | 20.9 | **53.6** |

**Table 7. Proportion of statistics selection across classification trees (pctle=percentile)**

| Crown area 50th pctle | Crown area variance | Mean TM b5 | Crown roundness variance | Mean TM b4 | Crown length 50th pctle | Crown area |
|---|---|---|---|---|---|---|
| 71.4% | 49.3% | 44.1% | 42.8% | 24.6% | 15.6% | 13% |
| **Crown length 25th pctle** | **Crown roundness 25th pctle** | **Crown roundness** | **Crown length variance** | **Mean TWI** | **Aspect** | **Crown area 25th pctle** |
| 6.5% | 3.9% | 1.3% | 1.3% | 1.3% | 1.3% | 1.3% |

**Table 8. Accuracies (%) of the QuickBird two-class fusion cases with the Maximum credibility decision rule.**

| | Black spruce | White spruce | Lodgepole pine | Trembling aspen | Overall accuracy |
|---|---|---|---|---|---|
| **QuickBird Aspect** | 100 | 43.2 | 64 | 70.4 | **69.4** |
| **QuickBird Fire date** | 100 | 10.4 | 0 | 15.9 | **31.6** |
| **QuickBird Slope** | 3.2 | 77.2 | 36 | 0 | **29.1** |
| **QuickBird TWI** | 100 | 18.5 | 0 | 65.9 | **46.1** |
| **QuickBird Landsat** | 96.7 | 26.5 | 88 | 70.4 | **70.4** |

**Table 9. Accuracies (%) of the QuickBird two-class fusion cases with the Maximum plausibility decision rule.**

| | Black spruce | White spruce | Lodgepole pine | Trembling aspen | Overall accuracy |
|---|---|---|---|---|---|
| **QuickBird Aspect** | 0 | 38.9 | 16 | 13.6 | **17.1** |
| **QuickBird Fire date** | 61.3 | 7.4 | 0 | 2.3 | **17.7** |
| **QuickBird Slope** | 3.2 | 53 | 8 | 0 | **16** |
| **QuickBird TWI** | 0 | 17.3 | 0 | 13.6 | **7.7** |
| **QuickBird Landsat** | 96.8 | 22.8 | 88 | 70.4 | **69.5** |

**Table 10. Accuracies (%) of the Landsat two-source fusion cases with the Maximum credibility decision rule.**

| | Black spruce | White spruce | Lodgepole pine | Trembling aspen | Overall accuracy |
|---|---|---|---|---|---|
| **Landsat Aspect** | 90.3 | 22.8 | 88 | 75 | **69** |
| **Landsat Fire date** | 100 | 2.4 | 0 | 15.9 | **29.6** |
| **Landsat Slope** | 80.6 | 29 | 96 | 65.9 | **67.9** |
| **Landsat TWI** | 90.3 | 19.1 | 92 | 72.7 | **68.5** |
| **Landsat QuickBird** | 96.8 | 26.5 | 88 | 70.4 | **70.4** |

**Table 11. Accuracies (%) of the best n-source combinations.**

| | Black spruce | White spruce | Lodgepole pine | Trembling aspen | Overall accuracy |
|---|---|---|---|---|---|
| **3 source combinations** | | | | | |
| **QuickBird, Landsat, Aspect** | 96.8 | 24 | 88 | 72.7 | **70.4** |
| **QuickBird, Landsat, Slope** | 90.3 | 29.6 | 88 | 65.9 | **68.4** |
| **QuickBird, Landsat, TWI** | 96.8 | 19.7 | 80 | 72.7 | **67.3** |
| **Landsat, Slope, TWI** | 87.1 | 19.7 | 92 | 72.7 | **67.9** |
| **Landsat, Slope, Aspect** | 88 | 27 | 88 | 70.4 | **68.2** |
| **4 source combinations** | | | | | |
| **Landsat, Aspect Slope, Fire date** | 90.3 | 23.4 | 80 | 72.7 | **66.6** |
| **QuickBird, Landsat, Slope, Aspect** | 90.3 | 27.8 | 88 | 68.2 | **68.6** |
| **QuickBird, Landsat, Slope, TWI** | 93.5 | 21.6 | 80 | 70.4 | **66.4** |
| **5 source combinations** | | | | | |
| **QuickBird, Landsat, Slope, Aspect, TWI** | 96.8 | 23.5 | 72 | 72.8 | **66.2** |
| **6 source combination** | | | | | |
| **QuickBird, Landsat, Slope, Aspect, TWI, Fire** | 100 | 0.6 | 0 | 18.2 | **29.7** |

**Figures:**

**Fig. 1. Study area, with panchromatic QuickBird imagery overlaid by stand boundaries of Site 4**

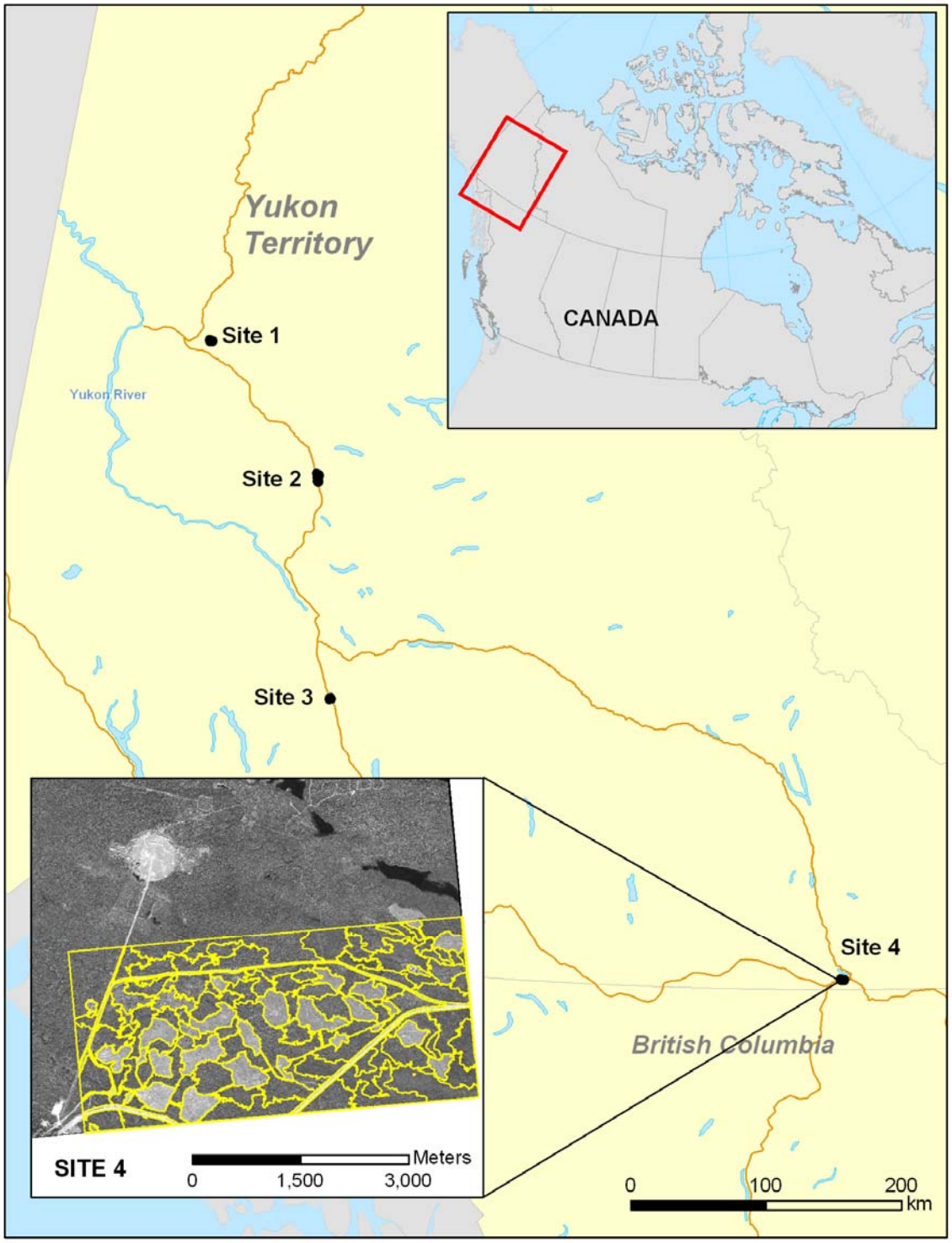

Fig. 2. (a) Stand delineation (white lines) with QuickBird imagery overlaid by ITC objects in forested segments in background. (b) Tree crown objects delineated with the ITC suite (in black).

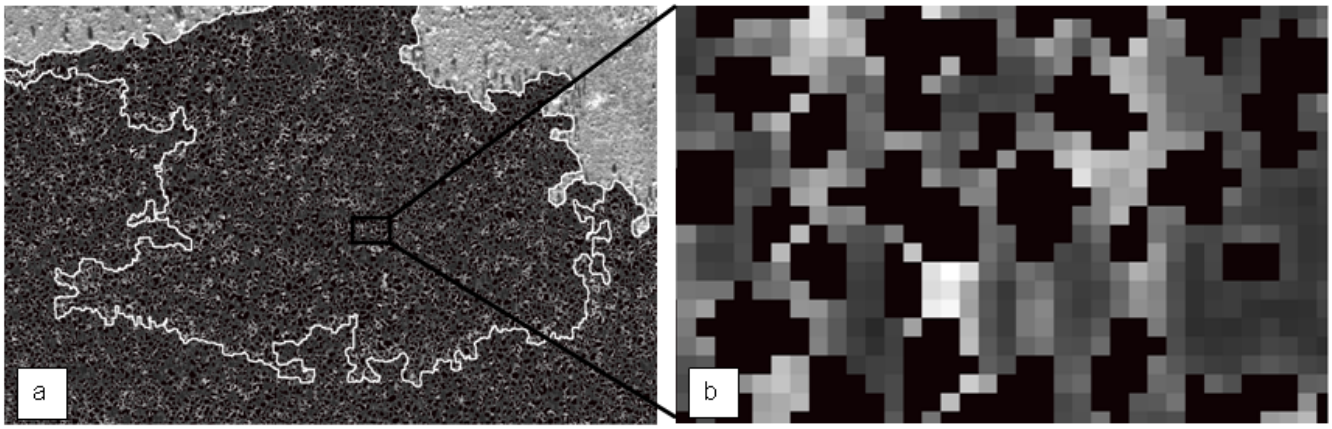


**Fig. 3. Mass function design principle for the union classes of QuickBird imagery, terrain aspect, slope and TWI sources.**

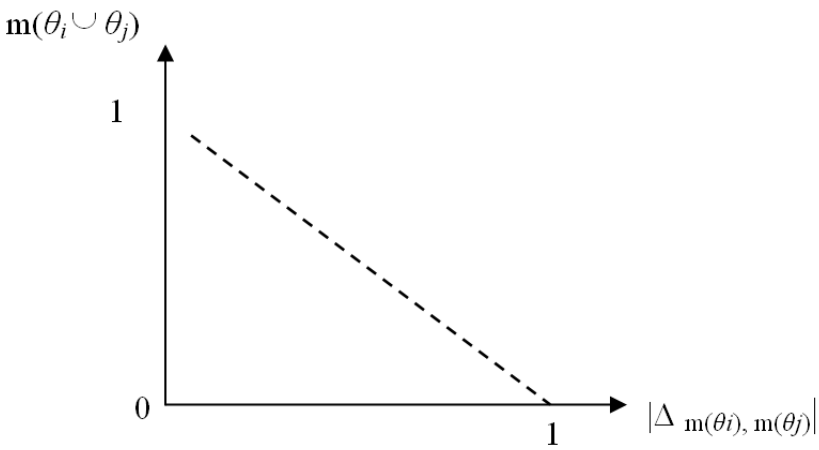

**Fig. 4. Mass functions for the terrain aspect.**

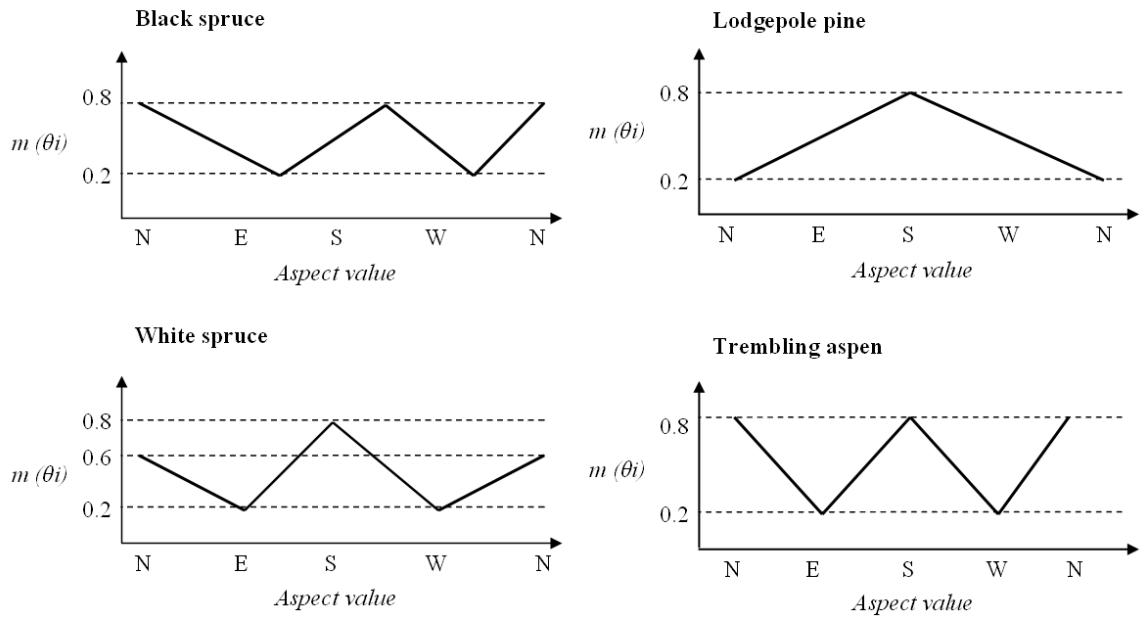


**Fig. 5. Mass functions for the slope.**